Preplasma effects on the emission directions of energetic electrons in relativistic laser–solid interactions

Y. Y. M A[1,2]†, Z. M. S H E N G[1], Y. T. L I[1], J. Z H A N G[1],
X. H. Y U A N[1], M. H. X U[1], Z. Y. Z H E N G[1], W. W. C H A N G[2],
M. C H E N[1] and J. Z H E N G[1]

[1]Laboratory of Optical Physics, Institute of Physics, Chinese Academy of Sciences,
Beijing 100080, People's Republic of China
[2]Department of Physics, National University of Defense Technology, Changsha 410073,
People's Republic of China

Abstract. Motivated by recent experimental observations of fast electron jets emitted along the target surface in intense laser–solid interactions with a large incident angle of the laser pulse, we simulate electron emissions by two-dimensional particle-in-cell simulations. When there is no preplasma in advance of the main laser pulse, electrons are emitted dominantly along the target surface. However, when there is preplasma, electron emission changes to the target normal. This difference originates from the different absorption mechanisms and different Coulomb electrostatic fields and self-generated magnetic fields induced in front of the target for the two cases.

1. Introduction

Fast electron production and transport have been studied extensively [1–5]. Fast electrons can be generated by different acceleration mechanisms, such as resonance absorption, vacuum heating, $J \times B$ heating, ponderomotive force acceleration, stochastic acceleration, and so on. However, there is still not enough understanding of physics mechanisms that control the emission directions of fast electrons. In the case of normal incidence of laser pulses, it is well known that the electron jets propagate normal into the target [2]. In the case of oblique incidence, electron jets are produced in the incident or specular reflection direction as a collimated beam when the preplasma is formed in front of the target [6]. The angular distribution of fast electrons during the interaction of an ultra-short intense laser pulse with solid targets has been studied by Sheng et al. [7], where the angular direction for fast electrons is given as a function of the particle's kinetic energy, experienced Coulomb potential changes, and the incident angle of the laser pulse. The effect of self-generated magnetic field has not been taken into account. Very recently, experiments have been conducted to study the effect of preplasma on fast electrons emission direction by Li et al. [8]. The experiments were performed with the 20 TW

† Present address: Laboratory of Optical Physics, Institute of Physics, Chinese Academy of Sciences, Beijing 100080, People's Republic of China.
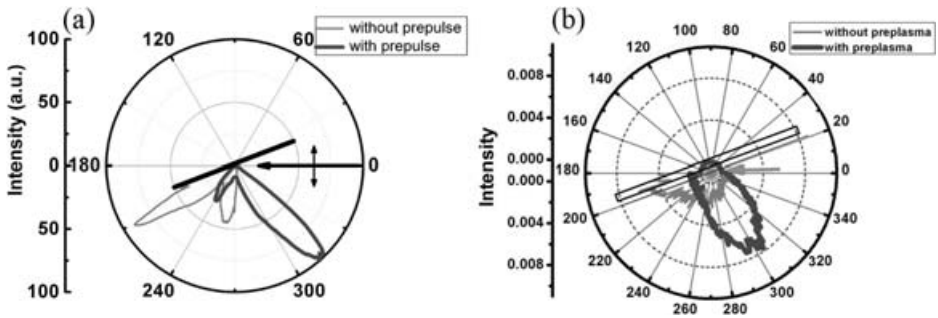
Figure 1. Angle distributions of fast electron emission observed (a) in experiments and (b) in simulations. The thin light-grey line is the angle distribution without prepulse. The thick dark-grey line is that with a prepulse.

laser eXtreme Light (XL-II) Ti:sapphire laser operating at 800 nm in the Institute of Physics, Chinese Academy of Sciences (CAS). The p-polarized laser beam was focused with an $f/3.5$ off-axis parabolic mirror onto a $30\,\mu$m thick aluminum target at an incident angle 60°. A 200 ps prepulse was introduced 0.5 ns before the main pulse in order to form the preplasma. Typical angular distributions of hot electrons with and without the prepulse are shown in Fig. 1. Electrons are emitted dominantly along the target surface if without prepulse and along the target normal if with prepulse. Experiments show that the fraction of electron emission along the target surface increases with the angle of incidence when it is changed from 30° to 70°. To explain the experimental observation, we investigate the effects of preplasma on the emission of fast electron by using two-dimensional (2D) particle-in-cell (PIC) simulations. The simulations show that there are different mechanisms of particle acceleration, different electric field and magnetic field structures for the cases with and without preplasma. The electron emission directions obtained in our simulations are qualitatively in agreement with the experimental observation.

2. Numerical simulation and analysis

The 2D-PIC code PLASIM [9, 10] has been used to simulate the fast electron emission. In the simulations, a solid target is irradiated by a 30 fs laser pulse obliquely with an incident angle 70°. The p-polarized laser is incident from the left boundary, whose electric vector is along the y-axis. The simulation box is $70\lambda_0 \times 70\lambda_0$. For the case without preplasma, the target is a uniform plasma slab at $6n_c$ in density and $4\lambda_0$ in thickness and $50\lambda_0$ in length. For the case with preplasma, the density changes linearly from zero to $6n_c$ in $15\lambda_0$. The laser intensity is $5 \times 10^{18}\,\mathrm{W\,cm^2}$. The incident laser pulse is in a Gaussian profile transversely with a beam waist of $10\,\mu$m. A total of 1024×1024 grids and 8 million particles are used in the simulation.

When there is no preplasma, the main mechanism for energetic electron generation is $J \times B$ heating [11]. This is shown in Fig. 2(a), where electrons are pulled out of the target by the electric field of the laser pulse and accelerated to the laser propagation direction. They are distributed regularly with a wavelength interval. Similar results can be found in [11], where electron bunches are observed to eject from the plasma walls with $1\lambda_0$ spacing. Since these electrons are pulled out by the
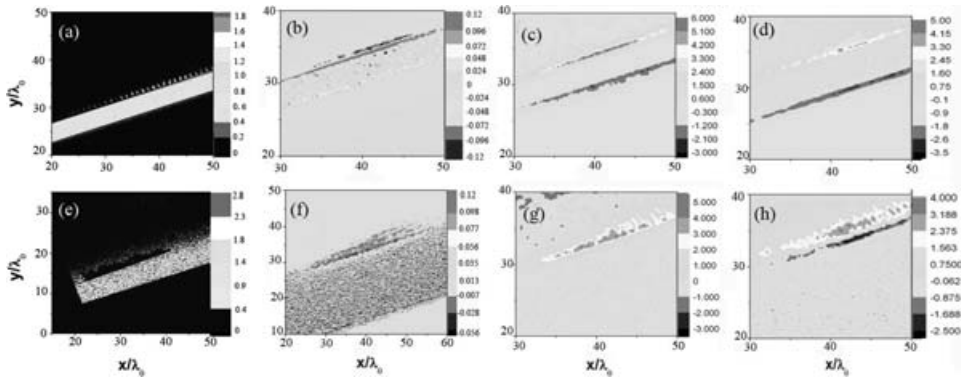
Figure 2. Contour plots of the electron energy density $\gamma n_{\mathrm{e}}/n_{\mathrm{c}}$ (a), (c) and current J_x (b), (f) in the x–y plane at $t = 290$ fs, where in (b) the lower and longer strip denotes backward currents and the upper and shorter strip denotes the forward currents formed by ejected electrons. Contour plots of quasi-static magnetic (c), (g) and electrostatic (d), (h) fields in the x–y plane at $t = 290$ fs. The first row is dedicated to the case without preplasma and the second row is the case with preplasma. The field is averaged in a laser cycle.

electric field of the laser near its positive peak, the neighboring bunches of electrons are separated by $1\lambda_0$.

Note that the fast electron currents move parallel to the target surface. The currents produced by forward-moving and backward-moving electrons form a current loop, which induces a quasi-static magnetic field around the target front as shown in Figs 2(c) and (g). At the same time, a strong charge separated field is also generated. When the magnetic field generated in front of target is intense enough, a significant fraction of fast electrons are reflected back to the vacuum by the magnetic field. However, the charge separation field will pull them back again. Therefore, these electrons are confined on the surface and account for the surface current. When there is preplasma in front of the target, the laser absorption mechanism and induced electrostatic field structures are very different (see Figs 2(d) and (h)]). Note that the electrostatic field is ambipolar at the target front, which is different from the unipolar field for the case without preplasma. In the presence of preplasma, the resonance absorption plays a key role in energetic electron production. An electron cavity (Fig. 2(e)) and the enhanced electric fields were observed near the critical surface of the target, which are typical characteristics of resonance absorption. Electrons in the cavity are expelled and piled up on both sides of the cavity. Since the incident laser is relativistic, electrons are accelerated also by the $J \times B$ mechanism in addition to resonance absorption.

The angular distribution of fast electrons in front of the target is shown in Fig. 1(b). In the case without preplasma, a fraction of fast electrons is emitted along the target surface. The electron current is also along the surface of the target, as shown in Fig. 2(b). Similar phenomena have also been found by Nakamura et al. [12]. However, in the case with preplasma, the emission peak of fast electrons moves to the target normal (shown in Fig. 1(b)). These results are in good agreement with our experiments shown in Fig. 1(a). We have also studied the effects of the time delay between the prepulse and main pulse on electron emission and found there are great differences for different delays. Generally, significant prepulse interaction

can result in large plasma scale lengths, which leads to the disappearance of the surface emission. Details about this will be discussed in another paper.

3. Conclusions

We have studied the effects of preplasma on the electron emission directions by 2D PIC simulations when an ultrashort laser pulse is incident obliquely at an angle of 70° onto a solid target. When there is no preplasma, electrons are emitted dominantly along the target surface. When there is preplasma, however, electron emission changes to the target normal. This difference originates from the different absorption mechanisms, different Coulomb electrostatic fields and self-generated magnetic fields induced in front of the target for different plasma density scale lengths. The simulations show qualitative agreement with the experimental results.

References

[1] Tabak, M. et al. 1994 Ignition and high gain with ultrapowerful lasers. *Phys. Plasmas* **1**, 1626–1634.

[2] Wilks, S. C. et al. 1992 Absorption of ultra-intense laser pulses. *Phys. Rev. Lett.* **69**, 1383–1386.

[3] Gremillet, L. et al. 1999 Time-resolved observation of ultrahigh intensity laser-produced electron jets propagating through transparent solid targets. *Phys. Rev. Lett.* **83**, 5015–5018.

[4] Norreys, P. A. et al. 1999 Observation of a highly directional γ-ray beam from ultrashort, ultraintense laser pulse interactions with solids. *Phys. Plasmas* **6**, 2150–2156.

[5] Gibbon, P. 1994 Efficient production of fast electrons from femtosecond laser interaction with solid targets. *Phys. Rev. Lett.* **73**, 664–667.

[6] Sentoku, Y. et al. 1999 Plasma jet formation and magnetic-field generation in the intense laser plasma under oblique incidence. *Phys. Plasmas* **6**, 2855.

[7] Sheng, Z.-M. et al. 2000 Angular distributions of fast electrons, ions, and bremsstrahlung X/γ-rays in intense laser interaction with solid targets. *Phys. Rev. Lett.* **85**, 5340–5343.

[8] Li, Y. T. et al. 2005 Submitted for publication.

[9] Ma, Y. Y. et al. 2002 2D3V dimensional particle simulation code for laser plasma interaction. *Chin. J. Comput. Phys.* **19**, 311 (in Chinese).

[10] Ma, Y. Y. et al. 2001 Particle simulation research on the detailed process of bubble generation. *Chin. Phys. Lett.* **18**, 1628.

[11] W. Kruer and Estabrook, K. 1985 $J \times B$ heating by very intense light. *Phys. Fluids* **28**, 430–432.

[12] Nakamura, T. et al. 2004 Surface-magnetic-field and fast-electron current-layer formation by ultraintense laser irradiation. *Phys. Rev. Lett.* **93**, 265002.